Acta Chemica Scandinavica, 1998: 52: 1285–1292
Printed in UK – all rights reserved

ACTA
CHEMICA SCANDINAVICA
ISSN 0904–213X

Reduction, Crystal Structure and Magnetic Properties of $Co_{3-x}Al_xO_{4-\delta}$ ($0.0 \leqslant x \leqslant 2.0$, $0.0 \leqslant \delta \leqslant 1.0$). Comparison with the Co/γ-Al_2O_3 Fischer–Tropsch Catalyst

Ole H. Hansteen,[a] Helmer Fjellvåg[a,*] and Bjørn C. Hauback[b]

[a]Department of Chemistry, University of Oslo, N-0315 Oslo, Norway and [b]Institutt for Energiteknikk, N-2007 Kjeller, Norway

Hansteen, O. H., Fjellvåg, H. and Hauback, B. C., 1998. Reduction, Crystal Structure and Magnetic Properties of $Co_{3-x}Al_xO_{4-\delta}$ ($0.0 \leqslant x \leqslant 2.0$, $0.0 \leqslant \delta \leqslant 1.0$). Comparison with the Co/γ-Al_2O_3 Fischer–Tropsch Catalyst. – Acta Chem. Scand. 52: 1285–1292. © Acta Chemica Scandinavica 1998.

Spinel type samples $Co_{3-x}Al_xO_4$ ($0.0 \leqslant x \leqslant 2.0$) were synthesized from citrate solutions and used as reference compounds for characterization of a 20% Co/γ-Al_2O_3 Fischer–Tropsch catalyst. With increasing Al content for the observed solid solution phase between Co_3O_4 and $CoAl_2O_4$, the unit cell expands smoothly, the antiferromagnetic ordering temperature decreases ($T_N \leqslant 40$ K), and the temperature required for reduction increases. Low-temperature reduction yields a partially reduced intermediate (Co^{II}) phase of the NaCl type. The crystal structure of such a partially reduced phase $(Co_{5/6}Al_{1/6})_{0.92}O$ has been determined on the basis of powder X-ray and neutron diffraction data: space group $Fm\bar{3}m$; a = 422.98(4) pm; R_{wp} = 4.0%, R_p = 3.1%. $(Co_{5/6}Al_{1/6})_{0.92}O$ orders antiferromagnetically below $T_N = 320 \pm 5$ K with a magnetic structure similar to that of CoO, $\mu_{AF} = 3.57(3)\ \mu_B$; R_M = 7.2%. TPR data for the oxidized catalyst show, consistent with PXD data, the presence of Co_3O_4 supported on γ-Al_2O_3. An additional mixed Co/Al oxide phase probably exists as an interface layer of $Co_{3-x}Al_xO_4$ with $x \approx 0.5$. The latter composition is consistent with the observed antiferromagnetic ordering temperature $T_N = 27 \pm 1$ K for the oxidized catalyst. The activated catalyst obtained on reduction at 573 K was found to consist of fine particles (28 nm) of ferromagnetic cobalt (*fcc*) together with a partially reduced, NaCl-type phase $(Co_{0.88}Al_{0.08})O$ supported on γ-Al_2O_3.

Cobalt supported on γ-Al_2O_3, usually promoted with noble metals such as rhenium, platinum and rhodium and also rare earth elements such as lanthanum, is an interesting catalyst for the synthesis of hydrocarbons by CO hydrogenation, the so-called Fischer–Tropsch synthesis. Cobalt is typically deposited in the oxidized state at the surface of γ-Al_2O_3. The catalyst is thereafter activated by reduction of di- and trivalent cobalt species to elementary Co(s) by means of hydrogen gas, preferably in the temperature range 573–673 K. Previous studies showed a complex reduction behavior for the oxidized Co/γ-Al_2O_3 catalyst, which was explained by a large degree of interaction at the interface between Co species and γ-Al_2O_3 during the catalyst preparation.[1] The interface reaction increases as a function of increasing calcination temperature due to a higher solid-state diffusion rate. Owing to this interface reaction major amounts of cobalt are left in an oxidized state after the activation process. In addition to the spinel-type Co_3O_4 and $CoAl_2O_4$ indications for mixed Co/Al oxides both in the oxidized and the activated catalyst have been reported.[1,2]

In the Co–Al–O system, three stoichiometric phases with spinel-type crystal structure are reported, Co_3O_4, Co_2AlO_4 and $CoAl_2O_4$. In the spinel type structure, AB_2O_4, the A and B atoms occupy, respectively, tetrahedral and octahedral holes in an *fcc* lattice of oxygen atoms (space group $Fd\bar{3}m$). Co_3O_4 has the normal spinel type structure with Co^{II} for A and Co^{III} for B.[3] Co_2AlO_4 and $CoAl_2O_4$ have partially inverse spinel-type structures with 27 and 15.5% of the A-position filled by trivalent Al atoms, respectively.[4,5] There are indications for a solid-state solution phase $Co_{3-x}Al_xO_4$ ($0.0 \leqslant x \leqslant 2.0$).[3,5] The stoichiometric Co spinels are antiferromagnetically ordered at lower temperatures, $T_N < 46$ K. In the paramagnetic state minor deviations from Curie–Weiss behavior have been explained in terms of a temperature independent contribution to the paramagnetic susceptibility.[3,6–8]

Comparative studies with closely related, single-phase model compounds are often required in order to extract information about the different phases in multi-phase

* To whom correspondence should be addressed.

specimens like the $Co/\gamma\text{-}Al_2O_3$ catalyst. Hence the present study focuses on detailed characterization, i.e. reduction, crystal structure and magnetic properties, of an extended number of model compounds with general composition $Co_{3-x}Al_xO_{4-\delta}$ ($0.0 \leqslant x \leqslant 2.0$, $0.0 \leqslant \delta \leqslant 1.0$). At the same time, similar studies are conducted for a (real) $Co/\gamma\text{-}Al_2O_3$ catalyst in order to approach an improved understanding of the nature of the Co/Al oxide interface layer, for the oxidized as well as for the reduced (activated) catalyst.

Experimental

Synthesis. Samples of spinel type $Co_{3-x}Al_xO_4$, $0.0 \leqslant x \leqslant 2.0$, were prepared from citrate solutions. The starting materials for the synthesis were $Al(NO_3)_3 \cdot 9H_2O$ (p.a., >98%, Fluka), $Co(CH_3COO)_2 \cdot 4H_2O$ (p.a., >99%, Fluka) and citric acid monohydrate, $C_3H_4(OH)(COOH)_3 \cdot H_2O$ (p.a., >99.8%, Riedel-de Haën). Gravimetric analyses were made for $Co(CH_3COO)_2 \cdot 4H_2O$ and $Al(NO_3)_3 \cdot 9H_2O$ prior to use. $Al(NO_3)_3 \cdot 9H_2O$ was initially dissolved in a melt of citric acid (weight ratio 1 : 5) and 3 ml distilled water. A clear solution was obtained after removal of nitrous gases by boiling. Thereafter, $Co(CH_3COO)_2 \cdot 4H_2O$ was added along with additional distilled water. The citrate solution was dehydrated at 450 K, and carbonaceous species in the resulting X-ray amorphous xerogel were removed by incineration at 720 K. The fine powder was cold-pressed into pellets, placed in an alumina crucible, and calcined in air at 1100 K for 48 h with one intermediate grinding followed by repelletization. The samples were slowly cooled to 570 K in the furnace before transferred to a desiccator. All samples were well crystalline powders with the exception of $CoAl_2O_4$, where a second calcination in air at 1300 K for 30 h was required. The colour of the samples, as seen by the naked eye, changed from black ($x = 0.0$) via green ($x = 0.5$, 1.0, 1.5) to blue ($x = 2.0$). The oxidized 20% $Co/\gamma\text{-}Al_2O_3$ catalyst was delivered by Statoil, Trondheim.*

Reductions. Isothermal reductions of $Co_{3-x}Al_xO_4$ and the 20% $Co/\gamma\text{-}Al_2O_3$ catalyst were performed in sealed silica glass ampoules using weighed chips of Zr (99.5% A. D. Mackay Inc.) as reducing agent (oxygen getter). The ampoules, with the samples, were repeatedly flushed with argon before evacuation and sealing in order to minimize the amount of gaseous oxygen in the system prior to the reduction. Zr was positioned in the warmer zone of the furnace at 873 K in order to assure complete oxidation to ZrO_2.[9] The sample temperature which was kept in the range 573–673 K typically used for catalyst activation, was controlled by varying the distance between the sample and Zr within the temperature gradient of the tube furnace. The ampoules were opened in an argon filled glovebox [$p(O_2)$ and $p(H_2O) < 1$ ppm]. Care was taken to assure inert atmosphere during storage, handling and subsequent characterization of specimens.

Temperature-programmed reduction (TPR) was performed by an AMI-1 Catalyst Characterization System from Altamira Instruments. The temperature program used for all samples included a pretreatment of the sample in Ar at 748 K for 15 min (gas flow rate 30 $cm^3\ min^{-1}$, heating rate 20 $K\ min^{-1}$) prior to the reduction performed on heating to 1173 K in $10\%H_2/Ar$ (gas flow rate 99 $cm^3\ min^{-1}$, heating rate 5 $K\ min^{-1}$). All gases were of purity >99.99% and they were further purified in a molecular sieve and a cold trap before use.

Characterization. Powder X-ray diffraction (PXD) data were collected by Guinier–Hägg cameras at 298 K using Si as internal standard ($a = 543.1065$ pm). Both Cr $K\alpha_1$ ($\lambda = 228.970$ pm, detection limit for impurities ca. 0.3 wt%)[10] and Cu $K\alpha_1$ ($\lambda = 154.0598$ pm) radiation were used. Unit cell dimensions were determined by least squares calculations using the program UNITCELL.[11] Synchrotron (SR) PXD data were collected for $(Co_{5/6}Al_{1/6})_{0.92}O$ ($Co_{3-x}Al_xO_{4-\delta}$, $x = 0.5$, $\delta = 0.75$) with the powder diffractometer in Debye–Scherrer mode at the Swiss Norwegian Beam Line (BM1) at ESRF (Grenoble). Monochromatic X-rays were obtained from a channel-cut Si(111) crystal. X-Rays of wavelength 110.103 pm were used. The sample was contained in a sealed and rotating glass capillary, diameter 0.5 mm. Intensity data were collected at 298 K between $2\theta = 20$ and 90° in steps of $\Delta(2\theta) = 0.03°$. Powder neutron diffraction (PND) data were collected for $(Co_{5/6}Al_{1/6})_{0.92}O$ with the two-axis powder diffractometer PUS at the JEEP II reactor, Kjeller (Norway). A cylindrical sample holder of vanadium, carefully sealed with an indium washer, was used. Monochromatized neutrons of wavelength 112.74 pm were obtained by reflection from Ge(711) of a focusing composite germanium monochromator. The scattered intensities were measured by two detector units, each containing a vertical stack of seven position-sensitive ^3He detectors which covers 20° in 2θ. Intensity data were collected at 10 K and 298 K between $2\theta = 10$ and 125° in steps of $\Delta(2\theta) = 0.05°$. The regions $2\theta = 27.65$–$29.10°$ (10 K) and $2\theta = 31.70$–$32.80°$ (10 and 298 K) were excluded in the analysis of the PND data due to additional scattering originating from the instrument. The GSAS program package[12] was used for Rietveld-type profile refinements of the powder X-ray and neutron diffraction data collected at 298 K. The background was modelled by cosine Fourier series polynomials for both data sets. The peak shape of the PXD(SR) and PND patterns were modelled by a pseudo-Voigt function. The scattering lengths $b_{La} = 8.27$ fm, $b_{Co} = 2.53$ fm and $b_O = 5.81$ fm were taken from the GSAS library. For profile refinement of the PND data collected

* The 20% $Co/\gamma\text{-}Al_2O_3$ catalyst sample delivered by Statoil Research Center, Trondheim (Norway) had been prepared by incipient wetness impregnation of a $\gamma\text{-}Al_2O_3$ support (Puralox, Cordea, B-5207) with an aqueous solution of $Co(NO_3)_2 \cdot 6H_2O$ (p.a., 99%, Fluka) and calcined at 648 K in air after drying.

at 10 K (crystal and magnetic structure) the Fullprof program[13] was used. The following parameters were varied for the PXD(SR) data and PND data (in parentheses); 1 (1) scale factor, 1 (1) zero point, 5 (5) profile parameters, 1 (1) unit cell dimension, 2 (2) isotropic displacement factors, 17 (12) background parameters. In total, 27 (20) free variables entered into the least-squares refinements. 11 (18) Bragg reflections contributed to the observed profile consisting of 2333 (2300) data points. For the PND data at 10 K two magnetic components were refined in addition.

Thermogravimetric analysis (TGA) was performed with a Perkin Elmer TGA7. Data reduction was performed with standard programs for the systems.

Magnetic susceptibility data were measured by a Quantum Design SQUID-magnetometer (MPMS) in the temperature range 2–300 K for magnetic fields (H) up to 50.0 kOe. All samples were zero field cooled and the temperature dependence of the magnetic susceptibility was measured on heating. The air-sensitive, reduced samples were held in evacuated and sealed spherical silica glass ampoules, whereas gelatine capsules were used for all other samples. The measured magnetic susceptibility was corrected for diamagnetic contribution from the sample container and from core electrons.

Results and discussion

PXD characterization

The $Co_{3-x}Al_xO_4$ model samples were well crystalline and gave sharp Bragg reflections in the PXD data which were indexed according to the cubic spinel-type structure, space group $Fd\bar{3}m$. The variation in the unit cell dimensions (Fig. 1) strongly indicates complete miscibility between the two end phases, Co_3O_4 and $CoAl_2O_4$, of the spinel series $Co_{3-x}Al_xO_4$ ($0.0 \leqslant x \leqslant 2.0$). The relative intensity of certain reflections changes with the aluminium content (x) and can possibly be used as a separate measure for composition. For example, the PXD patterns for $x = 1.5$ and 2.0 appear slightly different compared to the remaining samples, e.g. with no intensity for (111).

The unit cell expands gradually upon increasing aluminium content (x) (Fig. 1). The modest expansion (0.79%) can be interpreted in terms of ionic radii for the substituting elements. Ionic radii, according to Shannon,[14] are $r_{tetr}(Al^{III}) = 39$, $r_{oct}(Al^{III}) = 53.5$, $r_{oct}(Co^{III}, LS) = 54.5$, $r_{tetr}(Co^{II}, HS) = 58$ and $r_{oct}(Co^{II}, HS) = 74.5$ pm. Al^{III} substitutes for low-spin $Co^{III}(LS, d^6)$ in $Co^{II}Co^{III}_{2-x}Al^{III}_xO_4$. There is almost no size difference between the tabulated values for these substituting atoms. Furthermore, the literature indicate that a partial inversion of the spinel-type structure may occur for $x > 0.0$.[4,5] This implies that some $Co^{II}(HS)$ will be randomly distributed over octahedral sites and some Al^{III} will be located on tetrahedral sites. For such a partial inversion, a minor unit cell expansion may be expected on the basis of the ionic radii. The observed unit cell expansion is probably

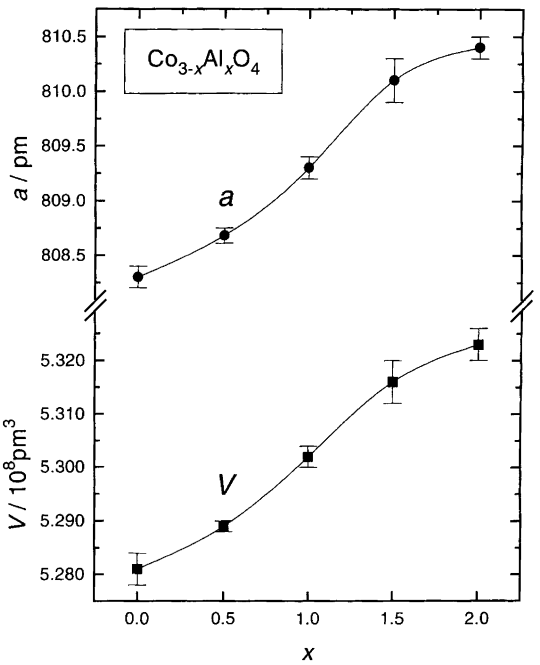

Fig. 1. Unit cell dimensions for cubic spinel-type $Co_{3-x}Al_xO_4$ with $0.0 \leqslant x \leqslant 2.0$ at 298 K.

a combined effect of substitution of Al^{III} for $Co^{III}(LS)$ and partial inversion of the spinel-type structure.

The PXD pattern for the 20% Co/γ-Al_2O_3 catalyst shows weak and broad reflections which corresponds to the patterns for $Co_{3-x}Al_xO_4$ ($x = 0.0$, 0.5, 1.0). From the center positions of the broad reflections $a = 808.2(4)$ pm is derived. This corresponds well to the value for Co_3O_4 (Fig. 1). If the broad reflections are a result of composition fluctuations in a spinel-type solid solution, one may derive unit cell dimensions in the range 806.9–809.4(4) pm. However, the lower value of these is too small (cf. Fig. 1), and it is more likely that the broadening is caused by small particle size. If so, an average particle size of 42 ± 4 nm for this spinel phase is estimated on the basis of the Scherrer formula for particle size broadening. Nevertheless, the existence of poorly crystalline $Co_{3-x}Al_xO_4$ with varying but low Al content at the interface between the γ-Al_2O_3 support and Co_3O_4 can not be excluded on the basis of the PXD data.

Temperature programmed reduction. TPR studies of $Co_{3-x}Al_xO_4$ show that the onset temperature for reduction rise gradually with increasing aluminium content (x) (Fig. 2). Furthermore, several steps (peaks) appear in the TPR curves for $Co_{2.5}Al_{0.5}O_4$, Co_2AlO_4 and $Co_{1.5}Al_{1.5}O_4$ suggesting a stepwise reduction from Co^{III} via Co^{II} to Co(s). The stepwise reduction behavior is most prominent for $Co_{2.5}Al_{0.5}O_4$, whose TPR curve can be roughly divided into two separate peaks. The area confined under the TPR curve corresponds to the amount of hydrogen consumed during the reduction. The ratio between the areas of the two TPR peaks for $Co^{II}Co^{III}_{1.5}Al^{III}_{0.5}O_4$ is 32/100. This corresponds closely

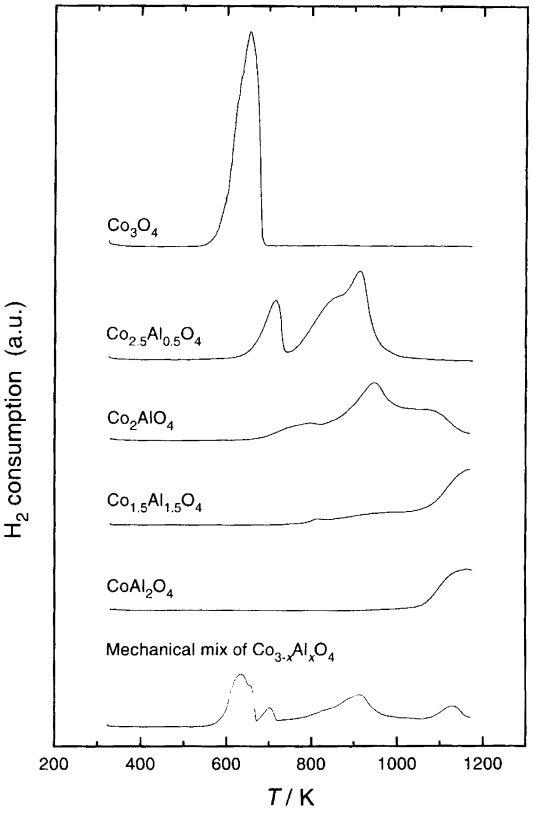

Fig. 2. TPR results for $Co_{3-x}Al_xO_4$ ($0.0 \leqslant x \leqslant 2.0$). Heating rate 5 K min^{-1}.

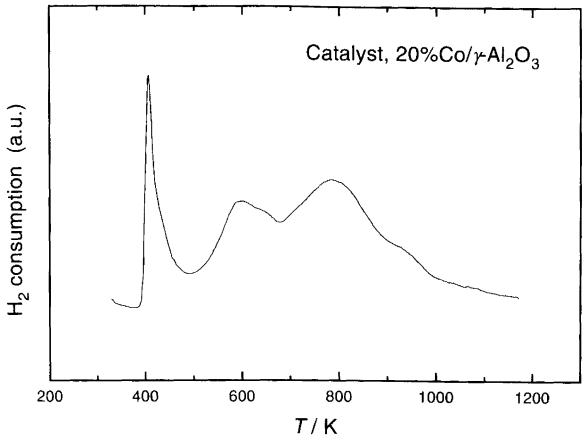

Fig. 3. TPR results for the 20% Co/γ-Al_2O_3 catalyst. Heating rate 5 K min^{-1}.

to the theoretical 30/100 ratio for the hydrogen consumption in a two-step reduction path from Co^{III} via Co^{II} to Co^0. Hence, the results for the $Co_{3-x}Al_xO_4$ model compounds clearly indicate the existence of a distinct, partially reduced intermediate phase, $Co^{II}{}_{3-x}Al_xO_{4-\delta}$. The consecutive reduction of the intermediate phase gives rise to a separate TPR peak. Earlier and present TPR data for Co_3O_4 show only one broad peak, which implies that reduction signals from Co_3O_4 and CoO overlap completely. On that basis it has been generally assumed that the partially reduced phases formed during stepwise reduction from Co^{III} via Co^{II} to Co could not be resolved by TPR.[1] The present study on $Co_{3-x}Al_xO_4$ shows definitely that the intermediate state can be resolved. In this way $Co_{3-x}Al_xO_4$ shows some resemblance to the $LaCoO_3$ perovskite, where TPR exhibits several separable peaks owing to formation of vacancy ordered, partially reduced intermediate phases.[9,15,16] The TPR results for $Co_{3-x}Al_xO_4$ in Fig. 2 show that complete reduction into Al_2O_3 and Co(s) requires an increase in temperature from 700 K ($x=0.0$) to about 1000 K ($x=0.5$) when small amounts of aluminium enters into the cobalt spinel.

Interpretation of the complex TPR curve observed for the oxidized 20% Co/γ-Al_2O_3 catalyst (Fig. 3) requires data for suitable reference materials, e.g. like those given above for $Co_{3-x}Al_xO_4$. The first, sharp TPR peak for the catalyst at 407 K (15% of the total reduction) is attributed to H_2-assisted decomposition of Co-nitrate species which are not decomposed during the calcination.[1] Several broad, overlapping peaks in the temperature range 500–1173 K suggests a complex reduction process. From comparison with model data, it is likely that the peak in the range 500–700 K (30% of the total reduction) corresponds to reduction of Co_3O_4 which is consistent with the PXD results for the oxidized catalyst. The sparse crystal structure data for γ-Al_2O_3 describes it as a cation defect spinel ($a=791$ pm), where Al^{III} randomly occupies 2/3 of the normally filled tetrahedral sites in addition to the octahedral sites.[17] Hence, γ-Al_2O_3 ($Al_{2/3}Al_2O_4$) and $CoCo_{2-x}Al_xO_4$ are structurally closely related. The cobalt atoms may fill and substitute on the tetrahedral and octahedral sites in γ-Al_2O_3. Therefore a reaction at the interface between γ-Al_2O_3 and deposited cobalt species (e.g. Co_3O_4) is expected, which probably leads to a spinel-type Co/Al oxide interface layer. If the temperature was sufficient for solid-state diffusion, one would expect growth of the interface layer, favouring spinel-type $Co_{3-x}Al_xO_4$ with a smooth increase in x from the Co-rich to the Al-rich side of the interface layer. The reduction process for such $Co_{3-x}Al_xO_4$ interface materials will probably resemble that of inhomogenous, bulk $Co_{3-x}Al_xO_4$ with a broad TPR peak above 700 K. This fits in fact the observations for the 20% Co/γ-Al_2O_3 catalyst between 700–1173 K (about 55% of its total reduction); see Fig. 2, where TPR data for a mechanical mixture of equal amounts of $Co_{3-x}Al_xO_4$ with $x=0.0$, 0.5, 1.0, 1.5, 2.0 are included for purpose of comparison. Although the calcination and reduction temperatures adopted for catalyst preparation ($T<700$ K) are too low for solid-state diffusion,[1] TPR shows that a reaction layer of $Co_{3-x}Al_xO_{4-\delta}$ must have been formed, the growth possibly progressing locally by help of produced reaction heat. In this respect the high dispersion of cobalt on the surface of γ-Al_2O_3 after impregnation enhances reactivity via the large contact area. The formation of cation defect Co/Al phases structurally analogous to γ-Al_2O_3 cannot be neglected;

however, no data on such phases are at hand. According to the TPR results for the catalyst, a reduction limited to 700 K leave major amounts of cobalt in a catalytically less active, oxidized state.

Reduced intermediate phases, $Co_{3-x}Al_xO_{4-\delta}$. The TPR experiments (Fig. 2) indicate the formation of an intermediate phase $Co_{3-x}Al_xO_{4-\delta}$ [alternatively written $(Co,Al)_{1-y}O$] upon reduction of Co^{III} to Co^{II}. Samples of nominal composition CoO ($x=0.0$, $\delta=1.00$), $Co_{2.5}Al_{0.5}O_{3.25}$ ($x=0.5$, $\delta=0.75$), and $Co_2AlO_{3.5}$ ($x=1.0$, $\delta=0.50$) were prepared by isothermal reduction at 673 K of $Co_{3-x}Al_xO_4$ with $x=0.0$, 0.5, 1.0, respectively. PXD showed that the samples of CoO and $Co_{2.5}Al_{0.5}O_{3.25}$ are single phase and adopts the cubic NaCl-type structure, space group $Fm\bar{3}m$. Sharp PXD reflections (Guinier–Hägg) for CoO indicates a well crystalline phase with $a=426.3(1)$ pm, which corresponds closely to literature data.[18] The PXD reflections (Guinier–Hägg) for $Co_{2.5}Al_{0.5}O_{3.25}$ are rather broad, $a=422.4(3)$ pm. In order to emphasize the relation to the NaCl-type structure, $Co_{2.5}Al_{0.5}O_{3.25}$ should be rewritten as $(Co_{5/6}Al_{1/6})_{0.92}O$, having probably a high concentration of cation vacancies. The oxygen content of $(Co_{5/6}Al_{1/6})_{0.92}O$ was confirmed by thermogravimetric analysis (Fig. 4), where subsequent PXD analysis assured complete reoxidation back to the $Co_{2.5}Al_{0.5}O_4$ spinel phase. For the sample with nominal composition $Co_2AlO_{3.5}$ [$(Co_{2/3}Al_{1/3})_{0.86}O$] PXD data show one spinel-type phase [$a=809.7(4)$ pm] and a NaCl-type phase $(Co,Al)_{1-y}O$ [$a=416(1)$ pm, broad reflections]. The two-phase situation indicates that the solid solubility range for aluminium in CoO has been exceeded. The cubic unit cell contracts considerably when Al^{III} substitutes for Co^{II} in CoO (cf. ionic radii above). The Al/Co ratio of the $(Co,Al)_{1-y}O$ phase of the nominal $Co_2AlO_{3.5}$ sample must be close to 1/2 as judged from the small unit cell dimension of this phase compared to those for CoO and $(Co_{5/6}Al_{1/6})_{0.92}O$. The unit cell for the spinel phase corresponds approximately to $Co_{1.75}Al_{1.25}O_4$. [$x=1.25$, cf. Fig. 1. The absence of (111) is another indication for $x>1.0$.] The fact that the observed spinel phase has $x<2.0$ implies that Co^{III} atoms exists in the structure. Since there are no indications for incomplete oxidation of the zirconium (reducing agent), the average oxidation state for cobalt in the nominal $Co_2AlO_{3.5}$ sample is considered to be 2.0. Hence, some Co(s) ought to be precipitated, and the reduced, nominal $Co_2AlO_{3.5}$ sample consists of three phases. This was confirmed by magnetic susceptibility data, which showed a weak ferromagnetic behavior (see below).

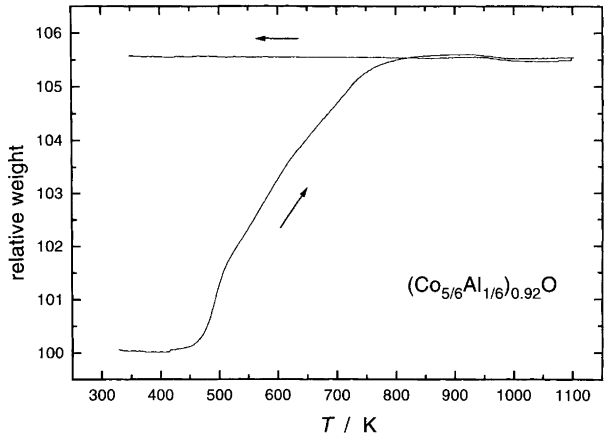

Fig. 4. Thermogravimetric data for oxidation of $(Co_{5/6}Al_{1/6})_{0.92}O$ in air. Heating rate 5 K min^{-1}.

Crystal structure of the reduced intermediate phase $(Co_{5/6}Al_{1/6})_{0.92}O$. Powder synchrotron X-ray and neutron diffraction data were collected at 298 K for $(Co_{5/6}Al_{1/6})_{0.92}O$. No peak splitting was resolved for the unusually broad Bragg reflections in the synchrotron experiments (Fig. 5). Separate Rietveld profile refinements for the PXD(SR) data and PND data were performed on the basis of the NaCl-type structure for $(Co_{5/6}Al_{1/6})_{0.92}O$; space group $Fm\bar{3}m$ with Co and Al in 4*a* (0, 0, 0) and O in 4*b* (½, ½, ½). Since variation of the occupation numbers for Co and Al did not improve the refinement (*R*-factors), they were fixed to the nominal

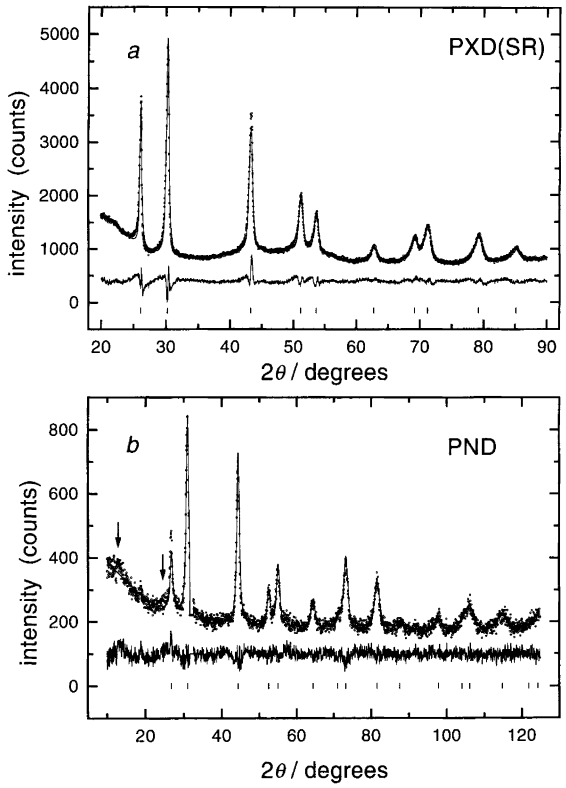

Fig. 5. (a) Synchrotron PXD ($\lambda=110.103$ pm) and (b) PND ($\lambda=112.74$ pm, excluded region $2\theta=31.70$–$32.80°$) profiles for $(Co_{5/6}Al_{1/6})_{0.92}O$ at 298 K. Experimental points marked by open circles, full line marks calculated profile, and lower full line marks difference plot. Vertical bars mark positions for Bragg reflections, and arrows mark traces of reflections of magnetic origin.

values 0.769 and 0.154, respectively. For the PXD(SR) data $a=422.98(4)$ pm ($R_{wp}=4.0\%$, $R_p=3.1\%$), whereas $a=423.23(8)$ pm ($R_{wp}=6.6\%$, $R_p=5.2\%$) for the PND data (the PXD and PND samples stemmed from different batches). Isotropic displacement factors (in 10^4 pm^2) are B(Co,Al)$=1.21(8)$ and B(O)$=1.09(5)$. The structural model gives a quite reasonable fit to the observed data, as shown by the calculated and difference diffraction profiles in Fig. 5.

For the PXD(SR) data the full width at half maximum (FWHM) is 0.34(1)° at $d=243.81$ pm, (111). This value contrasts that for a well crystalline and ordered phase like the perovskite oxide $LaCoO_3$ with FWHM$=$ 0.028(2)° for (104) at $d=268.70$ pm as well as for its reduced, vacancy-ordered derivatives $La_3Co_3O_8$ and $La_2Co_2O_5$.[9,16] Reduction of the perovskite proceeds topotactically, i.e. leaving the cationic sublattice intact, whereas an ordered arrangement of oxygen vacancies form on the oxygen sublattice. However, the reduction mechanism for the $Co_{3-x}Al_xO_4$ spinel-type oxide is different, since the removal of oxygen atoms from the solid phase requires considerable mass redistribution in order to retain the *fcc*-lattice of oxygen atoms in the reduced NaCl-type $(Co,Al)_{1-y}O$ phase. Furthermore, the cations are shifted from tetrahedral to octahedral interstices. Examination of scanning electron micrographs showed that the (macroscopic) particle size distribution remains essentially constant during the reduction. Since the reductions are carried out at low temperatures, the products do probably not represent an equilibrium situation. Hence, particle strain or inhomogenous Al/Co distribution are possible sources for the peak-broadening, together with a possible location of Al atoms in tetrahedral interstices in the reduced NaCl-type $(Co,Al)_{1-y}O$ phase. However, the PXD(SR) and PND data showed no evidence for such interstitial (cation Frenkel) defects.

Characterization of the activated catalyst. The oxidized 20% Co/γ-Al_2O_3 catalyst was activated by reduction at 573 K for 12 h by using Zr as an oxygen getter (heating/cooling rate 1 K min^{-1}). Two phases were identified by PXD at room temperature. One of the phases is elementary cobalt, predominantly in the cubic (*fcc*) high-temperature form, with only barely detectable amounts of an additional hexagonal (low-temperature) form in some samples. This contrasts the situation after reduction of bulk Co_3O_4 at $T<620$ K, which gives the hexagonal modification.[18] On the other hand, a small particle size is reported to favour the cubic form of cobalt.[19] The present cobalt particles in the activated catalyst are small, approximately 28 ± 5 nm as estimated from the Scherrer formula for particle size broadening of PXD reflections. The second phase in the activated catalyst is of $(Co,Al)_{1-y}O$-type (see above) with $a=424.5(1)$ pm. Its unit cell dimension indicates an aluminium content $x=$ 0.23(4). This indicates that the interface layer of the reduced catalyst consists of a partially reduced intermediate NaCl-type phase of composition $Co^{II}_{0.88}Al^{III}_{0.08}O$.

Magnetic properties. Figure 6 shows that the temperature dependence of the inverse magnetic gram susceptibility, $\chi_g^{-1}(T)$, for $Co_{3-x}Al_xO_4$ ($x=0.0$, 0.5, 1.0, 1.5, 2.0) obeys the Curie–Weiss law at temperatures above the respective ordering temperatures, T_N. The samples $Co_{3-x}Al_xO_4$ with $0.0\leqslant x\leqslant1.5$ exhibit a minimum in $\chi_g^{-1}(T)$ at low temperatures, indicating long-range antiferromagnetic ordering. The ordering temperatures (T_N) given in Table 1 agree with available literature data.[3,6,7] The present $\chi_g^{-1}(T)$ data for $CoAl_2O_4$ show no indication for magnetic order and agree in that sense with literature reports on a poorly defined minimum in $\chi_g^{-1}(T)$ around 4 K and weak indications for antiferromagnetic peaks in PND at 4 K.[7]

The magnetic susceptibility data for the oxidized 20% Co/γ-Al_2O_3 catalyst in Fig. 6 refer to the cobalt-containing part (i.e. mainly Co_3O_4, estimated to around 27 wt%) after correction for diamagnetic contribution

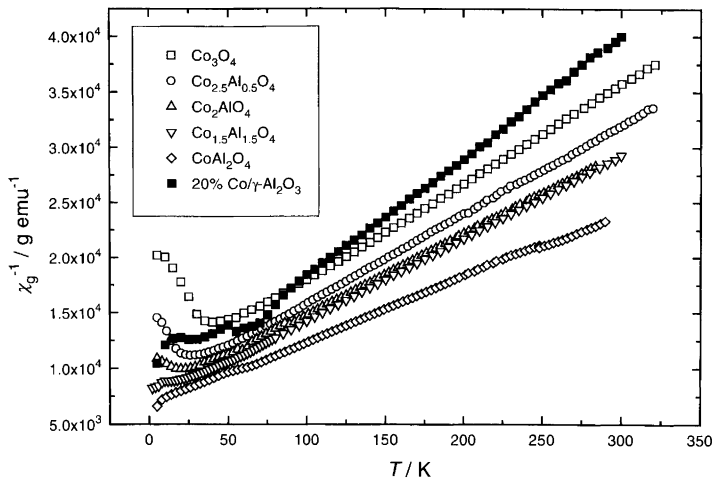

Fig. 6. Temperature dependence of the inverse magnetic susceptibility (χ_g^{-1}) for $Co_{3-x}Al_xO_4$ ($0.0\leqslant x\leqslant2.0$) and the oxidized 20% Co/γ-Al_2O_3 catalyst.

Table 1. Antiferromagnetic ordering temperatures, T_N, for $Co_{3-x}Al_xO_4$ ($0.0 \leqslant x \leqslant 2.0$) and oxidized 20% $Co/\gamma\text{-}Al_2O_3$ catalyst.

	T_N/K[a]
Co_3O_4	40
$Co_{2.5}Al_{0.5}O_4$	26
Co_2AlO_4	20
$Co_{1.5}Al_{1.5}O_4$	12
$CoAl_2O_4$	—
$20\%Co/\gamma\text{-}Al_2O_3$	27

[a] T_N is taken as minimum in $\chi_g^{-1}(T)$.

from (unreacted) $\gamma\text{-}Al_2O_3$. The anomaly in $\chi_g^{-1}(T)$ between 50 and 80 K is most probably due to an antiferromagnetic transition in adsorbed oxygen, as supported by corresponding test experiments on Co_2AlO_4 (Fig. 7), where the marked cusp in $\chi_g(T)$ almost completely disappeared after repeated flushing of the sample chamber with helium gas.

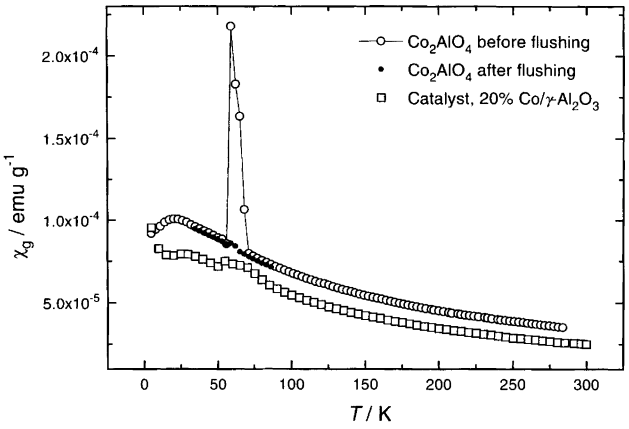

Fig. 7. Comparison of magnetic susceptibility for the 20% $Co/\gamma\text{-}Al_2O_3$ catalyst (squares) with that for Co_2AlO_4 prior (open circles) and after (filled circles) removal of surface oxygen by repeated flushing with helium.

The minimum in $\chi_g^{-1}(T)$ at 27 ± 1 K for the oxidized 20% $Co/\gamma\text{-}Al_2O_3$ catalyst indicates long range antiferromagnetic ordering for a spinel-type $Co_{3-x}Al_xO_4$ phase with aluminium content slightly less than $x = 0.5$. Hence, low temperature magnetic susceptibility data appear to be an additional valuable tool in characterization of the oxidized catalyst. For the activated catalyst $\chi_g(T)$ data show the presence of ferromagnetic cobalt. Although PXD suggest an average particle size as small as 28 ± 5 nm, the catalyst does not exhibit superparamagnetic behaviour at 298 K [M(H) hysteresis is observed].

The approximately temperature-independent magnetic susceptibility for the nominal $Co_2AlO_{3.5}$ sample (inset to Fig. 8), and the relatively high χ_g-values compared to those for $(Co_{5/6}Al_{1/6})_{0.92}O$, indicates the presence of small amounts of ferromagnetic Co(s) in the sample after reduction. This ferromagnetic cobalt completely dominates the measured magnetic susceptibility. Hence, no para- or antiferromagnetic contributions to the magnetic susceptibility from the $(Co,Al)_{1-y}O$ phase are detectable.

Powder neutron diffraction data for $(Co_{5/6}Al_{1/6})_{0.92}O$ at 10 K show a number of additional reflections of magnetic origin (Fig. 9). Their intensities gradually decrease on increasing temperature (Fig. 10). There is still minor magnetic scattering into (111), (113) and (311) at 298 K (see arrows in Fig. 5; Miller indices refer to the magnetic unit cell). The antiferromagnetic ordering temperature $T_N = 320 \pm 5$ K is estimated by extrapolation of the integrated intensity for (111) to the background level (Fig. 10). The magnetic susceptibility data for $(Co_{5/6}Al_{1/6})_{0.92}O$ in Fig. 8 refer then to the antiferromagnetic state. The additional magnetic reflections could be indexed on a slightly tetragonally distorted unit cell ($F4/m12/m$, non-standard setting of

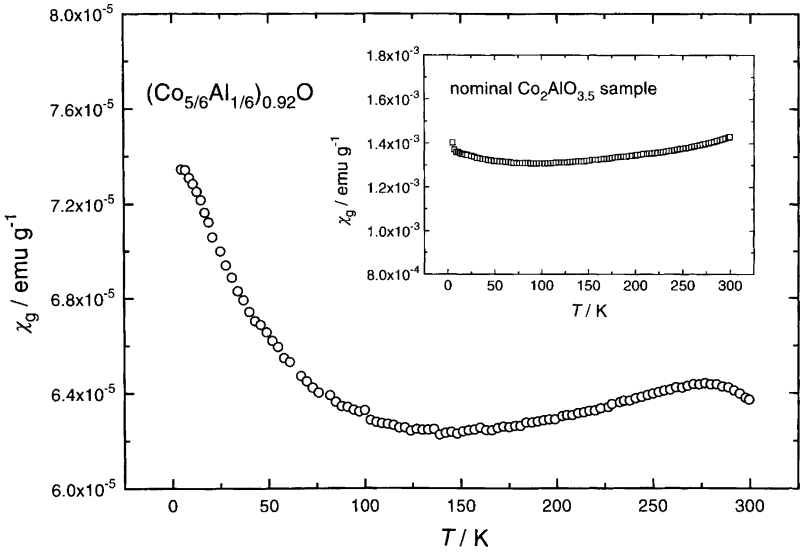

Fig. 8. Magnetic susceptibility for $(Co_{5/6}Al_{1/6})_{0.92}O$. Inset shows magnetic susceptibility for the three phase, nominal $Co_2AlO_{3.5}$ sample [$(Co_{2/3}Al_{1/3})_{0.86}O$].

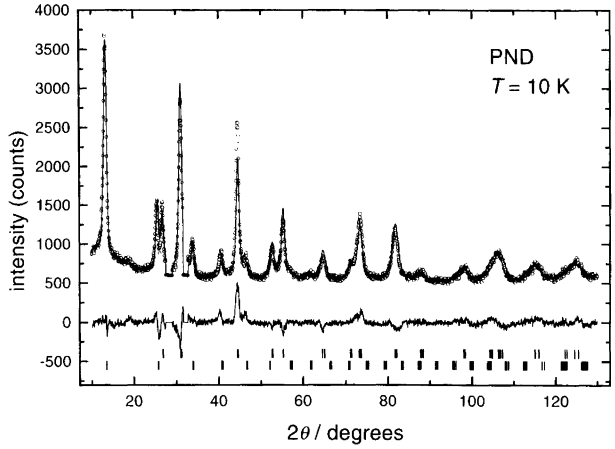

Fig. 9. PND profile at 10 K for $(Co_{5/6}Al_{1/6})_{0.92}O$ (λ = 112.74 pm). Experimental points are marked by open circles, full line marks calculated profile, and lower full line marks difference plot. Vertical bars mark positions for Bragg reflections of crystallographic (upper row) and magnetic origin (lower row). Two regions are excluded due to additional scattering originating from the instrument (2θ = 27.65–29.10 and 31.70–32.80°).

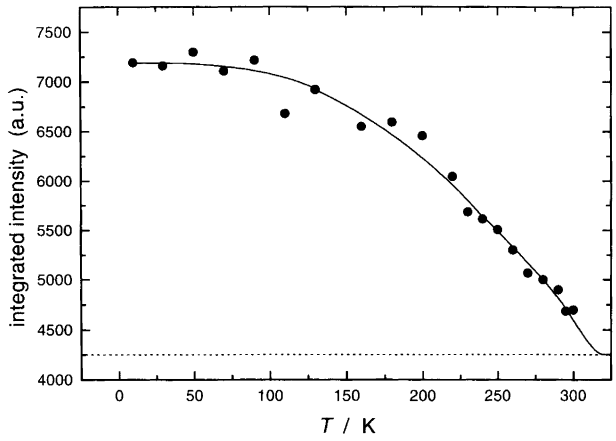

Fig. 10. Temperature dependence of integrated PND intensity for the magnetic (111) for $(Co_{5/6}Al_{1/6})_{0.92}O$. The dashed line represents the background level. The fully drawn line is a guide to the eye.

space group *I*4/*mmm*); $a = 846.2(3)$ pm, $c = 841.0(5)$ pm; $R_{wp} = 7.1\%$, $R_p = 5.0\%$. The unit cell and magnetic structure is similar to that of CoO ($T_N = 291$ K, $\mu_{AF} = 3.80\ \mu_B$).[20] The refined magnetic moment is $\mu_{AF} = 3.57(3)\ \mu_B$, with components $\mu_\perp = 1.45(9)\ \mu_B$ and $\mu_\parallel = 3.27(6)\ \mu_B$; $R_M = 7.2\%$. Figure 9 shows the observed, calculated and difference diffraction profile (10 K) for $(Co_{5/6}Al_{1/6})_{0.92}O$.

Acknowledgement. This work has received financial support from the Research Council of Norway. The skilful assistance from the project team at the Swiss–Norwegian Beam Line, ESRF is gratefully acknowledged. Statoil Research Center is acknowledged for providing the catalyst sample and for kindly placing its TPR apparatus at our disposal.

References

1. Arnoldy, P. and Moulijn, J. A. *J. Catal. 93* (1985) 38.
2. Moen, A., Nicholson, D. G., Clausen, B. S., Hansen, P. L., Molenbroek, A. and Steffensen, G. *Chem. Mater. 9* (1997) 1241.
3. Roth, W. L. *J. Phys. Chem. Solids 25* (1964) 1.
4. Garcia Casado, P. and Rasines, I. *J. Solid State Chem. 52* (1984) 187.
5. Toriumi, K., Ozima, M., Akaogi, M. and Saito, Y. *Acta Crystallogr., Sect. B34* (1978) 1093.
6. Blasse, G. *Philips Res. Rep. 18* (1963) 383.
7. Roth, W. L. *J. Phys. Rad. 25* (1964) 507.
8. Cossee, P. and van Arkel, A. E. *J. Phys. Chem. Solids 15* (1960) 1.
9. Hansteen, O. H., Fjellvåg, H. and Hauback, B. C. *J. Mater. Chem. In press.*
10. Gilbu, B., Fjellvåg, H. and Kjekshus, A. *Acta Chem. Scand. 48* (1994) 37.
11. Nolång, B. *Program UNITCELL*, Department of Chemistry, Uppsala University, Sweden.
12. Larson, A. C. and Von Dreele, R. B. *Program GSAS, General Structure Analysis System*, LANSCE, MS-H 805, Los Alamos National Laboratory, Los Alamos, NM.
13. Rodriguez-Carvajal, J. *FULLPROF, a Program for Rietveld Refinement and Pattern Matching Analysis*, Abstr. of the Satellite Meeting on Powder Diffraction of the XV Congress of the IUCR, 1990, p. 127.
14. Shannon, R. D. *Acta Crystallogr., Sect. A32* (1976) 751.
15. Gilbu Tilset, B., Fjellvåg, H. and Kjekshus, A. *J. Solid State Chem. 119* (1995) 271.
16. Hansteen, O. H., Fjellvåg, H. and Hauback, B. C. *J. Solid State Chem. In press.*
17. Knözinger, H. and Ratnasamy, P. *Catal. Rev. 17* (1978) 31.
18. Emmett, P. H. and Shultz, J. F. *J. Am. Chem. Soc. 51* (1929) 3249.
19. Owen, E. A. and Jones, D. M. *Proc. Phys. Soc. B67* (1954) 456.
20. Roth, W. L. *Phys. Rev. 110* (1958) 1333.

Received April 2, 1998.